HHS Public Access

Author manuscript

Mol Pharm. Author manuscript; available in PMC 2015 June 05.

Published in final edited form as:

Mol Pharm. 2012 September 4; 9(9): 2669–2676. doi:10.1021/mp3002232.

Polyvalent Dendrimer-Methotrexate as a Folate Receptor-Targeted Cancer Therapeutic

Thommey P. Thomas[#*,†,‡], **Baohua Huang**[#†,‡], **Seok Ki Choi**[#†,‡], **Justin E. Silpe**[‖], **Alina Kotlyar**[†,‡], **Ankur M. Desai**[†,‡], **Hong Zong**[†,‡], **Jeremy Gam**[†,‡], **Melvin Joice**[†,‡], and **James R. Baker Jr.**[†,‡]

[†]Michigan Nanotechnology Institute for Medicine and Biological Sciences, University of Michigan, Ann Arbor, Michigan 48109, United States

[‡]Department of Internal Medicine, University of Michigan, Ann Arbor, Michigan 48109, United States

[‖]Department of Macromolecular Science and Engineering, University of Michigan, Ann Arbor, Michigan 48109, United States

[#] These authors contributed equally to this work.

Abstract

Our previous studies have demonstrated that a generation 5 dendrimer (G5) conjugated with both folic acid (FA) and methotrexate (MTX) has a higher chemotherapeutic index than MTX alone. Despite this, batch-to-batch inconsistencies in the number of FA and MTX molecules linked to each dendrimer led to conjugate batches with varying biological activity, especially when scaleup synthesis was attempted. Since the MTX is conjugated through an ester linkage, there were concerns that biological inconsistency could also result from serum esterase activity and differential bioavailability of the targeted conjugate. In order to resolve these problems, we undertook a novel approach to synthesize a polyvalent G5–MTX_n conjugate through click chemistry, attaching the MTX to the dendrimer through an esterase-stable amide linkage. Surface plasmon resonance binding studies show that a G5–MTX_{10} conjugate synthesized in this manner binds to the FA receptor (FR) through polyvalent interaction showing 4300-fold higher affinity than free MTX. The conjugate inhibits dihydrofolate reductase, and induces cytotoxicity in FR-expressing KB cells through FR-specific cellular internalization. Thus, the polyvalent MTX on the dendrimer serves the dual role as a targeting molecule as well as a chemotherapeutic drug. The newly synthesized G5–MTX_n conjugate may serve as a FR-targeted chemotherapeutic with potential for cancer therapy.

[*]**Corresponding Author**: Rm. 4039 BSRB, MNIMBS,109 Zina Pitcher Place, University of Michigan, Ann Arbor, MI 48109. Tel: 734-615-1569. Fax: 734-615-2506. thommey@umich.edu..

ASSOCIATED CONTENT

Supporting Information

^{1}H NMR spectra, UPLC profiles, binding curves, and cytotoxicity results. This material is available free of charge via the Internet at http://pubs.acs.org.

The authors declare no competing financial interest.

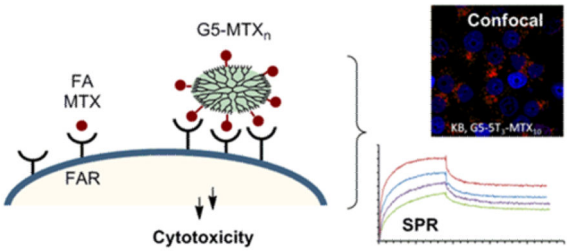

Keywords

dendrimer; nanoparticle; methotrexate; drug delivery; cancer

INTRODUCTION

Nanoparticle-based targeted drug delivery carries several advantages over conventional chemotherapy, including specificity, solubility, increased retention time, and enhanced target drug concentration.[1-3] Despite the recent explosion in the production of cancer nanotherapeutics, the application of most of these approaches in clinical studies has suffered significant setbacks.[4] One of the reasons for this is the difficulty in producing consistent, large-scale batches of homogeneous multifunctional molecules (e.g., with a targeting molecule and a drug), a problem that is exacerbated when multiple functionalities (e.g., a targeting molecule and a drug) are conjugated onto the surface of the nanoparticle.[5] Therefore, further improvements in the design and synthesis of nanotherapeutics is crucial for synthesizing clinically viable multifunctional drug conjugates. One of the ways this can be achieved is by designing nanoparticles with a single molecule serving dual functions (e.g., that serves both as a receptor targeting molecule and a chemotherapeutic drug).

Dendrimers are nanoscale macromolecules extensively used for targeted drug delivery owing to their biocompatibility and the presence of large numbers of peripheral functional groups that allow polyvalent conjugation of multiple molecules.[6-9] Dendrimers have been extensively utilized for delivering drugs and imaging agents.[9-18] We initially utilized folic acid (FA) as a ligand for synthesizing generation 5 (G5) dendrimer conjugates to target cells exhibiting folate receptor (FR) overexpression in several tumor types, for the delivery of chemotherapeutic drugs such as the antifolate methotrexate (MTX).[19] Importantly, our prior studies have shown that FR cell targeting of a "G5–FA$_m$–MTX$_n$" conjugate resulted in improved chemotherapeutic index as compared to free MTX.[20-23] In order to synthesize the G5–FA$_m$–MTX$_n$ we employed a complex, multistep, sequential synthesis that included the partial acetylation of the surface amino groups, coupling of FA through amide linkages, glycidolation of remaining free amino groups, and finally conjugation of the MTX through ester linkages.[21] This complex process allowed the synthesis of reproducible small-scale (milligram to gram scale) batches of material that showed consistent *in vitro* and *in vivo* efficacy. However, when we attempted to synthesize the kilogram-scale batches necessary for clinical trial studies, we found that the final product was chemically and biologically inconsistent. Our analyses have shown that a major limitation in these molecules is varying numbers of FA and MTX on the dendrimer.[5,24] This observation is supported by our studies

suggesting that less than 5% of the synthesized G5–FA_4–MTX_5 contained the desired number of 4 FA and 5 MTX.[5]

We sought to resolve these consistency limitations in FR-targeted MTX dendrimer conjugates by two different strategies: first, we simplified the synthesis by using MTX itself to target the FR (although at a ~20- to 100-fold lower affinity compared to FA),[25] by exponentially increasing binding avidity through polyvalent interactions from the dendrimer conjugated MTX molecules.[26-28] Second, the MTX was conjugated through a serum-stable amide linker, and via copper-free click chemistry. In addition, unlike shorter amide linkers,[22,29] we hypothesized that a long cyclooctyne-incorporated tether would facilitate binding to the DHFR, thereby enhancing MTX cytotoxicity. The objective of the study was to demonstrate the biological activity of a polyvalent G5–MTX_n nanoparticle in which the MTX serves as both a targeting agent and a chemotherapeutic drug.

Recently we reported the ability to synthesize a G5–MTX_n conjugate through copper-free click chemistry using a cyclooctyne-based linker.[30] We show by surface plasmon resonance (SPR) spectroscopy that the avidity of a synthesized G5–MTX_{10} conjugate to the surface-immobilized folate binding protein is increased >4000-fold over free MTX. This unique MTX conjugate also binds to FR-expressing KB cells in a receptor-specific manner, inhibits DHFR activity, and induces cell cytotoxicity.

MATERIALS AND METHODS

Materials

All solvents and chemicals were of reagent grade quality, purchased from Sigma-Aldrich (St. Louis, MO), and used without further purification unless otherwise noted. The G5-PAMAM dendrimer (G5-NH_2) was prepared at the Michigan Nanotechnology Institute for Medicine and Biological Sciences, University of Michigan, under a GMP-controlled environment. Dulbecco's phosphate-buffered saline (PBS) and other cell culture reagents were obtained from Gibco/BRL (Gaithersburg, MD). N_3-5-TAMRA (N_3-5T; excitation/emission wavelength = 540 nm/575 nm) was purchased from Click Chemistry Tools, LLC., (Macon, GA). KB, a subline of the cervical carcinoma HeLa cells, and B16-F10, a melanoma cell line, were obtained from ATCC (Manassas, VA).

Synthesis of G5–MTX_n and G5–$5T_m$–MTX_n

The G5–MTX_n conjugates (n = 5, 10, or 17) were synthesized as described previously.[30] In order to track the cellular uptake of the G5–MTX_n, we also synthesized additional bifunctional conjugates onto which the fluorescent dye 5T was also linked through click chemistry (G5–$5T_m$–MTX_n). The G5-$cyclooctyne_{20}$ (**1**, Scheme 1) was prepared as reported earlier by using 20 equiv of a cyclooctyne derivative[31] in the presence of PyBop.[30] ^{1}H NMR analysis of the product showed the presence of 20 cyclooctyne molecules per dendrimer.

Compound **1** underwent click chemistry reactions with γ-azido MTX at 5, 10, or 18 equiv to obtain G5–MTX_5, G5–MTX_{10}, and G5–MTX_{17}[30]. **1** (7.6 mg in 200 μL of methanol for each reaction) was also incubated with either 3 equiv of N_3-5T or 10 equiv of γ-azido MTX to produce G5–$5T_3$ **2** (6.8 mg; 86.6% yield) and G5–MTX_{10} **3**, (7.2 mg; 84.3%) respectively.

For these click reactions, a DMSO stock solution of the N_3-5T or γ-N_3-MTX was added to the methanol solution of **1** and the reaction mixtures were stirred at room temperature under argon overnight. To synthesize G5–$5T_3$–MTX_{10} **4** (6.8 mg; 85.5%), following the overnight reaction of **1** (6.8 mg in 180 μL of methanol) with the 3 equiv of N_3-5T, additional overnight incubation was performed with 10 equiv of the γ-azido MTX. All of the final products were fully neutralized by acetylation (average total of 92 groups per dendrimer) prior to the click conjugation as described.[30] The final products obtained were dried under vacuum to remove the methanol, and the residue (~100 μL) was redissolved in ~3 mL of PBS buffer (pH = 7.4) and filtered through an Amicon centrifugal filter (10K cutoff; centrifuged at 4,200 rpm for 25 min at 13 °C) to remove the residual DMSO. With the high efficiency of the copper-free click chemistry, no detectable amount of unreacted G5-cyclooctyne was present in the final products, which was confirmed by HPLC analysis and monitoring the eluent peaks at 210 nm (data not shown). The retentate was then subjected to similar centrifugal washes two more times with PBS, followed by six times with DI water. The final retentate was dissolved in water, transferred into glass vials, and lyophilized.

All of the conjugates and their intermediate reaction products were analyzed by MALDI-TOF and ^{1}H NMR. The number of 5T and MTX attached onto the dendrimer was obtained from the ^{1}H NMR analysis by integration of the methyl protons of the terminal acetyl groups to the aromatic protons in the 5T structure, or to the proton of the aromatic pteridine ring on the MTX, respectively (Figure S1 in the Supporting Information). The average molecular weights of the conjugates were derived from the peak value of the MALDI-TOF analysis.

Ultrahigh Performance Liquid Chromatography (UPLC) Analysis

UPLC was performed using a Waters Acquity Peptide Mapping System and the method established in our laboratory as described elsewhere.[28] A 3 μL aliquot of each of the conjugates (1 mg/mL stocks) was autoinjected onto the column, and the flow rate was maintained at 0.208 mL/min. The UPLC profiles of the synthesized conjugates G5–$5T_3$, G5–MTX_{10}, and G5–$5T_3$–MTX_{10} are shown in Figure S2 in the Supporting Information.

Surface Plasmon Resonance (SPR) Spectroscopy

The SPR experiments were performed in a Biacore X instrument (Pharmacia Biosensor AB, Uppsala, Sweden) essentially according to the method described elsewhere.[28,32] Folate binding protein (FBP, bovine milk; Sigma) was immobilized to a CM5 sensor chip following a standard amide coupling protocol.[26,33] The immobilization process of FBP on the chip resulted in an 11000 response unit (RU) equivalent to 11 ng/mm^2 of the FBP. SPR studies for the kinetics of FBP binding were carried out by injection of the ligand or dendrimer solutions, each prepared in HBS-EP buffer, at a flow rate of 20 μL/min (FA, MTX) or 10 μL/min. (G5–MTX_n conjugates). The analysis of binding kinetics was performed as reported earlier.[28,32,33] Kinetic binding parameters, the rate of association (k_{on}), and the rate of dissociation (k_{off}) were determined by fitting each binding curve separately, using nonlinear regression analysis as described.[34] The dissociation constant ($K_D = k_{off}/k_{on}$) determined for each dendrimer conjugate refers to a mean value obtained from multiple independent measurements (n = 7–8) per conjugate.

Dihydrofolate Reductase (DHFR) Assay

The DHFR assay was carried out using a kit from Sigma and performed according to the manufacturer's protocol. Briefly, recombinant human DHFR (1.1 μg/mL) was diluted in an assay buffer and added to a mixture of 60 μM NADPH and 50 μM DHF and different concentrations of the conjugate in a UV-compatible 96-well plate. The reaction was initiated by adding the enzyme, and the kinetics of the NADPH conversion to NADP was monitored spectrophotometrically at 340 nm for 5 min. The enzyme velocity was calculated from the slope of the linear portion of the time-kinetics data.

Cell Culture

The KB cells were grown as a monolayer cell culture in folate-deficient RPMI 1640 medium supplemented with 10% fetal bovine serum (FBS). The 10% FBS provided a folate concentration equivalent to that which is present in the human serum (~20 nM). The FR-negative B16-F10 cells were cultured in DMEM medium under similar conditions. All of the cells were maintained at 37 °C and 5% CO_2 in the presence of 100 U/mL penicillin and 100 mg/mL of streptomycin.

Flow Cytometry Analysis

The cellular binding of G5–$5T_3$–MTX_{10} was determined by flow cytometry analysis as previously described.[18] Cells were plated in 24-well plates at a density of 3×10^5 cells/plate in FA-free RPMI containing 10% FBS. Two days later, the cells were changed to be in FA-free RPMI (in the absence of serum), and treated with different concentrations of the conjugates at 37 °C. The cells were rinsed with PBS containing BSA (0.1%) to remove unbound material, and the fluorescence was determined using an Accuri flow cytometer (BD Accuri Cytometers, Ann Arbor, MI). The data were analyzed using Accuri software, with the mean FL2-fluorescence of 10,000 cells determined on a population gated for viable cells.

Confocal Microscopic Analysis

Cells were seeded at a density of 5×10^5 cells/plate on glass-bottomed culture dishes (Mattek, Ashland, MA) two days prior to the experiment. Cells were incubated with G5–$5T_3$–MTX_{10} in cell culture medium, rinsed with PBS, fixed with paraformaldehyde, and mounted using solution containing the nuclear stain 4,6′-diamidino-2-phenylindole (DAPI). Fluorescent signals were sequentially scanned on an Olympus Fluoview 500 confocal system with an Olympus IX-71 microscope and a 60× water objective to maximize signal separation. The DAPI and 5-T were excited with a 405 nm diode and 543 nm HeNe green lasers, respectively. The signals were measured sequentially through 430–460 (for DAPI), and 560 nm long pass (for 5-TAMRA) filters. The *z*-series were taken through representative samples at steps of 0.225 μm with Kalman averaging of the two frames.

XTT Cytotoxicity Assay

Cells were seeded in 96-well microtiter plates (3000 cells/well) in medium containing dialyzed serum. Two days after plating, the cells were treated with the dendrimer conjugates in the tissue culture medium for the indicated time periods. A colorimetric "XTT" (sodium 3-[1-(phenylaminocarbonyl)-3,4-tetrazolium]-bis(4-methoxy-6-nitro) benzene sulfonic acid

hydrate) assay (Roche Molecular Biochemicals, Indianapolis, IN) was performed, following the vendor's protocol. After incubation with the XTT labeling mixture, the microtiter plates were read on an ELISA reader (Synergy HT, BioTek) at 492 nm, with the reference wavelength at 690 nm.[22]

RESULTS

For cellular uptake studies we synthesized a polyvalent G5 PAMAM-conjugate of 10 molecules of the drug MTX and 3 molecules of the sensing dye 5T per dendrimer (G5–$5T_3$–MTX_{10}). For cytotoxicity studies we also synthesized G5–MTX_n (n = 5, 10, and 17) conjugates that lacked the dye molecule, as previously described.[30] The number of specific conjugated molecules per dendrimer was derived from ^{1}H NMR analysis (Figure S1 in the Supporting Information). The purity of the conjugates was tested by UPLC analysis, and was shown to have less than 1% of free ligands (Figure S2 in the Supporting Information).

SPR-based dose-dependent binding curves for dendrimer–MTX conjugates (G5–MTX_n; n = 0, 5 and 10) to the FBP surface are shown in Figure 1. A negative control (G5-Linker, without any MTX on it) did not show any significant binding to the FBP surface (Figure 1C). In contrast, the SPR sensorgram for either the G5–MTX_5 (Figure 1A) or the G5–MTX_{10} (Figure 1B) shows the concentration-dependent binding kinetics. To determine the dissociation constants (K_D) for G5–MTX_n on a quantitative basis, we utilized a nonlinear regression method that uses SPR data to estimate the kinetic rate constants (k_{on}, k_{off}),[34] as a result, the steady state dissociation constants (K_D) are summarized in Table 1. These results provide a measure of the relative binding strength of the G5–MTX_n to FBP.

The SPR sensorgram for each G5–MTX_n conjugate also shows markedly by slow dissociation, a hallmark for multivalent tight binding.[26,35,36] This dissociation constant is also in agreement with that of G5–$FA_{8.2}$, a multivalent dendrimer comparator presenting the FA ligand.[26] Each dissociation curve for G5–MTX_n (n = 5, 10) per concentration suggests that the dendrimer conjugate dissociates apparently in multiple phases, initially at a rapid off rate, and subsequently at slower off rates. For example, G5–MTX_5, upon injection at 5.0 μM, shows up to 62% of fractional desorption (RU_d/RU_a), and G5–MTX_{10}, under the identical condition, shows 39% of fractional desorption at the end of data collection when its dissociation appears to be still incomplete.

The ability of the G5–MTX_{10} to inhibit DHFR activity was evaluated using recombinant human DHFR. As shown in Figure 2, G5–MTX_{10} inhibited DHFR activity in a dose-dependent fashion. The cellular uptake of fluorescently labeled G5–$5T_3$–MTX_{10} conjugate was examined in FR-expressing KB cells by flow cytometry analysis. During a 4 h incubation, the conjugate bound to the KB cells in a dose-dependent fashion, and the binding was completely blocked by preincubation with excess free FA (Figure 3). Similar binding curves, although with higher fluorescence intensities, were obtained when incubations were performed for a time period of 20 h (Figure S3 in the Supporting Information). In contrast, under identical conditions, no significant binding was observed in the FR-negative B16-F10 cells. A fifty percent maximum saturation level was reached at around 30 nM, which is similar to that which was obtained previously for the binding of

fluorescently labeled G5–FA conjugates.[19,22,37] The control conjugate G5–5T failed to show any significant binding at 30 nM (Figure S3 in the Supporting Information, inset). Confocal microscopy analysis (Figure 4) showed cellular internalization and the presence of the G5–$5T_3$–MTX_{10} conjugate in the cytosolic compartment. A *z*-series analysis of confocal microscopic fluorescence of single cells confirmed the intracellular localization of the conjugate (data not shown). The confocal microscopic study also confirmed the prevention of binding and internalization in KB cells by free excess FA, as well as the absence of any cellular uptake of the G5–$5T_3$–MTX_{10} in the B16-F10 cells (Figure 4).

The synthesized G5–MTX_n conjugates induced cytotoxicity in a dose-dependent manner, whether the concentrations were based on conjugate (Figure 5) or MTX molar concentrations (Figure S4 in the Supporting Information). The G5–MTX_5 conjugate was comparatively less cytotoxic than the other two G5 conjugates with higher numbers of MTX. The G5–MTX_{17} was not completely aqueous soluble and showed similar cytotoxicity as the G5–MTX_{10}. Additional studies were conducted with the soluble G5–MTX_{10} conjugate to explore the specificity and efficacy of the conjugate. Although G5–MTX_{10} was cytotoxic in the FR-positive KB cells with maximal inhibition at 30–100 nM, the conjugate failed to show any cytotoxicity at concentrations up to 1000 nM in the FR-negative B16-F10 cells, whereas free MTX induced dose-dependent cytotoxicity in both cell lines (Figure 6). In KB cells, the G5–MTX_{10} (IC_{50} ~ 30 nM) was relatively more cytotoxic as compared to a control conjugate G5–FA_5–MTX_7[20,22] (IC_{50} ~ 60 nM; Figure 6, panel A). The G5–MTX_{10} showed similar cytotoxicity to a recently synthesized G5–FA_3–MTX_3 conjugate that used a triazine-based linker.[32] The time-dependent cytotoxicity of the G5–MTX_{10} was then determined in the KB cells by incubating the KB cells with the conjugates for different time intervals, followed by incubation in conjugate-free medium for up to 48 h. As shown in Figure S5 in the Supporting Information, the G5–MTX_{10} was cytotoxic at both 1 and 4 h. In contrast, although free MTX was cytotoxic when incubated for 4 h or more, it failed to show significant cytotoxicity during a 1 h incubation period.

DISCUSSION

The recent finding that an alkyne/azide 1,3-dipolar cycloaddition reaction is well suited for bioconjugations[31] prompted us to adapt this approach to synthesize the cyclooctyne-based dendrimer–MTX conjugate. This synthesis has several advantages. First, the copper-free click reaction does not need any coupling reagent and catalyst, making the desired product easier to purify and avoiding Cu, which is known to induce biotoxicity. Second, the reaction is very efficient and specific. Third, this method allows different types of azido-modified molecules (e.g., a drug, an imaging agent, etc.) to be conjugated onto the same dendrimer platform. Fourth, the long tether of the cyclooctyne moiety provides greater length and flexibility which may facilitate binding to its targets, the FR and DHFR. Fifth, the amide coupling of MTX to the dendrimer provides stability against hydrolysis by serum esterases. Our studies show that G5–MTX_n conjugates thus synthesized bind to FR through polyvalent interaction, inhibit DHFR, and induce cytotoxicity through FR-specific cellular internalization.

SPR spectroscopy is a well-established technique for studying the binding kinetics of analytes to biological surfaces on a real-time basis. It has been applied for multivalent ligand–receptor interactions, including FA-conjugated G5 PAMAM dendrimers.[28,35,36,38,39] The SPR binding data presented in Figure 1 and Table 1 clearly demonstrates the efficacy of the polyvalent interaction of the G5–MTX_n to FR. As an illustration, the dissociation constant estimated for G5–MTX_5 (K_D = 28 nM) suggests that its binding avidity is enhanced by a factor of 857 (multivalent binding enhancement = $\beta = K_D^{mono}/K_D^{multi}$), relative to a free MTX molecule (K_D = 24 μM, sensogram not shown). The K_D value of the higher-valent conjugate G5–MTX_{10} shows much higher avidity (K_D = 5.5 nM), with the β value of 4360. Of these two conjugates, G5–MTX_{10} shows greater avidity, which is attributed primarily to its slower off rate (k_{off}). This observation is fully consistent with the hypothesis that complete dissociation by a multivalent ligand occurs very slowly because the multiple MTX coupled to a single dendrimer have to dissociate simultaneously from multiple receptor sites.[35,36,40] In summary, the SPR study demonstrated that as compared to free MTX a dendrimer-based multivalent MTX conjugate binds much more tightly to multiple FR on the surface. It also suggests that FR-overexpressing cancer cells can be targeted using a multivalent MTX-based nanoparticle.

The DHFR inhibition study shows that the conjugate inhibits DHFR in a dose-dependent fashion; however, the conjugate was comparatively less cytotoxic than free MTX at concentrations above 30 nM. This could suggest a lower affinity for DHFR of MTX conjugated to the dendrimer, even if it is assumed that only one MTX molecule on each dendrimer can bind to a DHFR molecule. Despite an apparent 2-fold lower IC_{50} value of the conjugate vs free MTX, by taking into consideration the known 10^3- to 10^4-fold higher affinity of the enzyme for MTX vs FA,[41] it is anticipated that the conjugate would induce significant cytotoxicity. Although the MTX cytotoxicity is also a consequence of its action on other enzymes in the folate metabolic pathway, such as the thymidine synthase, these results show the ability of the intact conjugate to inhibit the DHFR, the interaction most crucial for inducing cytotoxicity.

The cellular uptake studies demonstrate that the G5–$5T_3$–MTX_{10} conjugate is taken up into cells in a receptor-specific fashion, based on the observations that the conjugate bound to the FR-expressing KB cells in a receptor-saturable fashion, and the binding was reversed by preincubation with excess free FA. As further evidence supporting the FR-specific cell targeting, the conjugate failed to bind in the FR-negative B16-F10 cells, and the control G5–$5T_3$ dendrimer failed to bind to the FR-expressing cells.

All G5–MTX_n conjugates were cytotoxic in the FR-expressing KB cells. Fifty percent growth inhibition of the G5–MTX_{10} occurred at ~30 nM, which was also the IC_{50} value for uptake. Polyglutamation of the MTX at its γ-carboxylic acid is known to prevent transport of MTX across the membrane by the reduced folate carrier.[42] Similarly, it is possible that the dendrimer conjugated to MTX through its γ-carboxyl group is not taken up via the RFC. The lack of role of RFC in the conjugate uptake is further demonstrated by the observation that G5–MTX_n conjugate is neither taken up nor cytotoxic in the B16-F10 cells (Figures 4, 6), whereas free MTX at 100-fold lower equivalent concentration is cytotoxic, obviously

due to its cellular entry via the RFC. Therefore, we believe that in these experiments all internalization of G5–MTX_n may predominantly be FR-mediated. Therefore, this suggests that the increased cytotoxicity of the G5–MTX_{10} over the G5–MTX_5 is likely a reflection of the higher avidity of the former for the FR, as predicted by our SPR study. As the G5–MTX_{17} was not completely aqueous soluble, the lack of a further increase in the cytotoxicity potency over the G5–MTX_{10} could be due to a decreased availability of the soluble form. The G5–MTX_{10} conjugate showed relatively higher cytotoxicity as compared to a FA-targeted "G5–FA_5–MTX_7" conjugate that we had synthesized previously.[20,22] Although the reason for this is not evident, it is possible that under the FA-free conditions used in the cytotoxicity assay, the FA present in the G5–FA_5–MTX_7 may reverse the cell growth-inhibition by MTX. This hypothesis is supported by our previous observation that a "G5–FA_3" conjugate acts as a cell growth-promoting agent under these conditions.[32] It should be noted that the MTX linked to the azide linker showed relatively lower cytotoxicity vs free MTX. The reason for this is not known, and further studies are required to discern if this is due to a decreased uptake or to reduced inhibition of folate metabolism.

The FR-specific uptake of the G5–MTX_{10} was clearly evident from the observation that the conjugate was not cytotoxic in the FR-negative B16-F10 cells. In these conditions, another FA-based comparator "G5–FA_3–MTX_3" conjugate in which the MTX was conjugated through ester linkage using a triazine-based linker[32] showed partial cytotoxicity in the B16-F10 cells but only at concentrations above 300 nM (Figure 6). Such low activity is probably due to some esterase-mediated release of free MTX occurring during the 72 h incubation in serum-containing medium. Kaminskas et al. have investigated the cytotoxicity of nanoparticles in which MTX was conjugated to pegylated polylysine dendrimer through a matrix metalloproteinase-cleavable peptide linker.[43] In the low FR-expressing HT1080 cell model, the conjugates showed cytotoxicity with IC_{50} values of approximately 2–40 μM MTX equivalents, whereas a control conjugate with the MTX conjugated through a stable amide linker showed insignificant cytotoxicity (IC_{50} = ~500 μM).[43] Unlike these studies in which the observed cytotoxicity of the cleavable construct was attributed to released MTX, the current study showing potent cytotoxicity in high FR-expressing KB cells (IC_{50} = 300 nM MTX equivalents) is consequent to the polyvalent interaction of the stable amide-linked conjugate through FR followed by inhibition of cytosolic enzymes by the intact conjugate, and this mode of enzyme inhibition by the intact MTX conjugate was already discussed in Figure 2. However, further studies are needed to confirm the intracellular stability of the amide bond. In another recent study, Jiang et al. reported the synthesis of polyvalent G4–MTX_{36} conjugate in which MTX molecules are attached directly to the fourth generation dendrimer without having any intervening spacer.[44] This conjugate has been shown to be cytotoxic in KB cells with IC_{50} values in the micromolar range; however, the FR-independent uptake and cytotoxicity of this conjugate was not determined.[44]

The G5–MTX_{10} showed cytotoxicity even during a short incubation time of 1 h followed by incubation in conjugate-free medium for 48 h, whereas the free MTX failed to show significant cytotoxicity under these conditions (Figure S5 in the Supporting Information). This is probably due to the tight binding, possibly in combination with the rapid uptake, of the polyvalent conjugate through the multiple FRs, even during the short incubation period.

This result is in contrast to the monovalent MTX, which requires a longer time to be taken up through the FR because of its low affinity in KB cells.[45] Long-term (≥4 h) incubations resulted in the increased cytotoxicity of free MTX as compared to the G5–MTX_{10}. This could be due to the continuous cellular accumulation of free MTX, accomplished through its preferred, yet low-(micromolar)-affinity RFC,[46] whereas the uptake of the G5–MTX_{10}, taken up exclusively through the high-affinity FR, might slow down over time due to receptor downregulation.[47] Despite the relatively lower *in vitro* cytotoxicity of the G5–MTX_{10}, the FR-mediated specific uptake of the G5–MTX_{10} makes this drug conjugate a potentially preferred chemotherapeutic over free MTX, due to its *in vivo* specificity for FR-overexpressing tumor cells. Based on our previous *in vivo* studies using G5–FA–MTX conjugates,[20] it is possible that there will be some undesired uptake of the conjugate also into FR-expressing tissues such as the kidney and liver. However, based on our SPR and cell-based studies, we anticipate that the G5–MTX_n will have tumoricidal potency similar to the G5–FA–MTX, without inducing any significant organ or animal toxicity.[20]

In conclusion, this study shows that a polyvalent G5–MTX_{10} conjugate, in which MTX serves as both a targeting ligand and a chemotherapeutic drug, binds to FBP with more than 4000-fold enhancement in avidity over free MTX. The amide-linked, intact MTX conjugate was taken up specifically by FR-expressing cells where it inhibited DHFR and induced cytotoxicity. Altogether these results suggest that G5–MTX_{10} may serve as a potent chemotherapeutic for FR-overexpressing tumors.[10] The conjugate may also serve as a therapeutic to target activated macrophages implicated in inflammatory diseases.[15]

Supplementary Material

Refer to Web version on PubMed Central for supplementary material.

ACKNOWLEDGMENTS

This project has been funded with funds from the National Cancer Institute, National Institutes of Health, under Award CA119409. This work utilized the Morphology and Image Analysis Core of the Michigan Diabetes Research and Training Center funded by NIH5P60 DK20572 from the National Institute of Diabetes & Digestive & Kidney Diseases. We thank Dr. Stephen I. Lentz for his skillful technical help in the confocal microscopic analysis. We also thank Professors Mark Banaszak Holl and Bradford G. Orr for assisting with the analysis of the SPR spectroscopy data.

REFERENCES

(1). Duncan R. Polymer conjugates as anticancer nanomedicines. Nat. Rev. Cancer. 2006; 6(9):688–701. [PubMed: 16900224]

(2). Haag R, Kratz F. Polymer therapeutics: Concepts and applications. Angew. Chem., Int. Ed. 2006; 45(8):1198–215.

(3). de Bono JS, Ashworth A. Translating cancer research into targeted therapeutics. Nature. 2010; 467(7315):543–9. [PubMed: 20882008]

(4). Davis ME, Chen Z, Shin DM. Nanoparticle therapeutics: an emerging treatment modality for cancer. Nat. Rev. Drug Discovery. 2008; 7(9):771–82.

(5). Mullen DG, Fang M, Desai A, Baker JR, Orr BG, Holl MMB. A Quantitative Assessment of Nanoparticle-Ligand Distributions: Implications for Targeted Drug and Imaging Delivery in Dendrimer Conjugates. ACS Nano. 2010; 4(2):657–70. [PubMed: 20131876]

(6). Tomalia DA, Naylor AM, Goddard WA. Starburst Dendrimers - Molecular-Level Control of Size, Shape, Surface-Chemistry, Topology, and Flexibility from Atoms to Macroscopic Matter. Angew. Chem., Int. Ed. Engl. 1990; 29(2):138–75.

(7). Nanjwade BK, Bechra HM, Derkar GK, Manvi FV, Nanjwade VK. Dendrimers: Emerging polymers for drug-delivery systems. Eur. J. Pharm. Sci. 2009; 38(3):185–96. [PubMed: 19646528]

(8). Tomalia DA, Reyna LA, Svenson S. Dendrimers as multi-purpose nanodevices for oncology drug delivery and diagnostic imaging. Biochem. Soc. Trans. 2007; 35:61–67. [PubMed: 17233602]

(9). Thomas, TP.; Shukla, R.; Majoros, IJ.; Myc, A.; Baker, JR, Jr.. Poly(amidoamine) Dendrimer-Based Multifunctional Nanoparticles. In: Mirkin, CA.; Niemeyer, CM., editors. Nanobiotechnology II: More Concepts and Applications. Wiley-VCH; 2007.

(10). Elnakat H, Ratnam M. Distribution, functionality an gene regulation of folate receptor isoforms: implications in targeted therapy. Adv. Drug Delivery Rev. 2004; 56(8):1067–84.

(11). Kamaly N, Kalber T, Thanou M, Bell JD, Miller AD. Folate receptor targeted bimodal liposomes for tumor magnetic resonance imaging. Bioconjugate Chem. 2009; 20(4):648–55.

(12). Leamon CP, Reddy JA. Folate-targeted chemotherapy. Adv. Drug Delivery Rev. 2004; 56(8): 1127–41.

(13). McNerny DQ, Leroueil PR, Baker JR. Understanding specific and nonspecific toxicities: a requirement for the development of dendrimer-based pharmaceuticals. Wiley Interdiscip. Rev.: Nanomed. Nanobiotechnol. 2010; 2(3):249–59. [PubMed: 20166124]

(14). Thomas TP, Choi SK, Li MH, Kotlyar A, Baker JR Jr. Design of riboflavin-presenting PAMAM dendrimers as a new nanoplatform for cancer-targeted delivery. Bioorg. Med. Chem. Lett. 2010; 20(17):5191–4. [PubMed: 20659800]

(15). Thomas TP, Goonewardena SN, Majoros IJ, Kotlyar A, Cao Z, Leroueil PR, Baker JR Jr. Folate-targeted nanoparticles show efficacy in the treatment of inflammatory arthritis. Arthritis Rheum. 2011; 63(9):2671–80. [PubMed: 21618461]

(16). Thomas TP, Shukla R, Kotlyar A, Liang B, Ye JY, Norris TB, Baker JR Jr. Dendrimer-epidermal growth factor conjugate displays superagonist activity. Biomacromolecules. 2008; 9(2):603–9. [PubMed: 18193839]

(17). Toffoli G, Cernigoi C, Russo A, Gallo A, Bagnoli M, Boiocchi M. Overexpression of folate binding protein in ovarian cancers. Int. J. Cancer. 1997; 74(2):193–8. [PubMed: 9133455]

(18). Zhang Y, Thomas TP, Desai A, Zong H, Leroueil PR, Majoros IJ, Baker JR. Targeted Dendrimeric Anticancer Prodrug: A Methotrexate-Folic Acid-Poly(amidoamine) Conjugate and a Novel, Rapid, “One Pot” Synthetic Approach. Bioconjugate Chem. 2010

(19). Quintana A, Raczka E, Piehler L, Lee I, Myc A, Majoros I, Patri AK, Thomas T, Mule J, Baker JR. Design and function of a dendrimer-based therapeutic nanodevice targeted to tumor cells through the folate receptor. Pharm. Res. 2002; 19(9):1310–6. [PubMed: 12403067]

(20). Kukowska-Latallo JF, Candido KA, Cao Z, Nigavekar SS, Majoros IJ, Thomas TP, Balogh LP, Khan MK, Baker JR Jr. Nanoparticle targeting of anticancer drug improves therapeutic response in animal model of human epithelial cancer. Cancer Res. 2005; 65(12):5317–24. [PubMed: 15958579]

(21). Majoros IJ, Thomas TP, Mehta CB, Baker JR. Poly(amidoamine) dendrimer-based multifunctional engineered nanodevice for cancer therapy. J. Med. Chem. 2005; 48(19):5892–9. [PubMed: 16161993]

(22). Thomas TP, Majoros IJ, Kotlyar A, Kukowska-Latallo JF, Bielinska A, Myc A, Baker JR Jr. Targeting and inhibition of cell growth by an engineered dendritic nanodevice. J. Med. Chem. 2005; 48(11):3729–35. [PubMed: 15916424]

(23). Majoros IJ, Williams CR, Becker A, Baker JR Jr. Methotrexate delivery via folate targeted dendrimer-based nanotherapeutic platform. Wiley Interdiscip. Rev.: Nanomed. Nanobiotechnol. 2009; 1(5):502–10. [PubMed: 20049813]

(24). Gillies ER, Frechet JMJ. Dendrimers and dendritic polymers in drug delivery. Drug Discovery Today. 2005; 10(1):35–43. [PubMed: 15676297]

(25). Jackman AL, Theti DS, Gibbs DD. Antifolates targeted specifically to the folate receptor. Adv. Drug Delivery Rev. 2004; 56(8):1111–25.

(26). Hong S, Leroueil PR, Majoros IJ, Orr BG, Baker JR, Holl MMB. The binding avidity of a nanoparticle-based multivalent targeted drug delivery platform. Chem. Biol. 2007; 14(1):107–15. [PubMed: 17254956]

(27). Joshi A, Vance D, Rai P, Thiyagarajan A, Kane RS. The design of polyvalent therapeutics. Chemistry. 2008; 14(26):7738–47. [PubMed: 18553325]

(28). Li MH, Choi SK, Thomas TP, Desai A, Lee KH, Kotlyar A, Banaszak Holl MM, Baker JR Jr. Dendrimer-based multivalent methotrexates as dual acting nanoconjugates for cancer cell targeting. Eur. J. Med. Chem. 2012; 47(1):560–72. [PubMed: 22142685]

(29). Gurdag S, Khandare J, Stapels S, Matherly LH, Kannan RM. Activity of dendrimer-methotrexate conjugates on methotrexate-sensitive and -resistant cell lines. Bioconjugate Chem. 2006; 17(2): 275–83.

(30). Huang B, Desai A, Zong H, Tang S, Leroueil P, Baker JR Jr. Copper-free click conjugation of methotrexate to a PAMAM dendrimer platform. Tetrahedron Lett. 2011; 52(13):1411–1414. [PubMed: 21383864]

(31). Ornelas C, Broichhagen J, Weck M. Strain-promoted alkyne azide cycloaddition for the functionalization of poly(amide)-based dendrons and dendrimers. J. Am. Chem. Soc. 2010; 132(11):3923–31. [PubMed: 20184364]

(32). Zong H, Thomas TP, Lee KH, Desai A, Li MH, Kotlyar A, Zhang Y, Leroueil P, Gam JJ, Banaszak Holl MM, Baker JR. Bifunctional PAMAM dendrimer conjugates of folic acid and methotrexate with defined ratio. Biomacromolecules. 2012; 13(4):982–91. [PubMed: 22360561]

(33). Plantinga A, Witte A, Li M-H, Harmon A, Choi SK, Banaszak Holl MM, Orr BG, Baker JR, Sinniah K. Bioanalytical Screening of Riboflavin Antagonists for Targeted Drug Delivery—A Thermodynamic and Kinetic Study. ACS Med. Chem. Lett. 2011; 2(5):363–7. [PubMed: 21686082]

(34). Ober RJ, Caves J, Sally Ward E. Analysis of exponential data using a noniterative technique: application to surface plasmon experiments. Anal. Biochem. 2003; 312(1):57–65. [PubMed: 12479835]

(35). Adler P, Wood SJ, Lee YC, Lee RT, Petri WA, Schnaar RL. High Affinity Binding of the Entamoeba histolytica Lectin to Polyvalent N-Acetylgalactosaminides. J. Biol. Chem. 1995; 270(10):5164–71. [PubMed: 7890626]

(36). Arranz-Plaza E, Tracy AS, Siriwardena A, Pierce JM, Boons GJ. High-Avidity, Low-Affinity Multivalent Interactions and the Block to Polyspermy in Xenopus laevis. J. Am. Chem. Soc. 2002; 124(44):13035–46. [PubMed: 12405830]

(37). Thomas TP, Ye JY, Chang YC, Kotlyar A, Cao Z, Majoros IJ, Norris TB, Baker JR. Investigation of tumor cell targeting of a dendrimer nanoparticle using a double-clad optical fiber probe. J. Biomed. Opt. 2008; 13(1):014024. [PubMed: 18315382]

(38). Gestwicki JE, Cairo CW, Mann DA, Owen RM, Kiessling LL. Selective Immobilization of Multivalent Ligands for Surface Plasmon Resonance and Fluorescence Microscopy. Anal. Biochem. 2002; 305(2):149–55. [PubMed: 12054443]

(39). Tassa C, Duffner JL, Lewis TA, Weissleder R, Schreiber SL, Koehler AN, Shaw SY. Binding Affinity and Kinetic Analysis of Targeted Small Molecule-Modified Nanoparticles. Bioconjugate Chem. 2010; 21(1):14–9.

(40). Mammen M, Choi SK, Whitesides GM. Polyvalent interactions in biological systems: implications for design and use of multivalent ligands and inhibitors. Angew. Chem., Int. Ed. 1998; 37:2755.

(41). Matthews DA, Alden RA, Bolin JT, Filman DJ, Freer ST, Hamlin R, Hol WG, Kisliuk RL, Pastore EJ, Plante LT, Xuong N, Kraut J. Dihydrofolate reductase from Lactobacillus casei. X-ray structure of the enzyme methotrexate. NADPH complex. J. Biol. Chem. 1978; 253(19):6946–54. [PubMed: 29045]

(42). Rosenblatt DS, Whitehead VM, Vera N, Pottier A, Dupont M, Vuchich MJ. Prolonged inhibition of DNA synthesis associated with the accumulation of methotrexate polyglutamates by cultured human cells. Mol. Pharmacol. 1978; 14(6):1143–7. [PubMed: 732812]

(43). Kaminskas LM, Kelly BD, McLeod VM, Sberna G, Boyd BJ, Owen DJ, Porter CJ. Capping methotrexate alpha-carboxyl groups enhances systemic exposure and retains the cytotoxicity of drug conjugated PEGylated polylysine dendrimers. Mol. Pharmaceutics. 2011; 8(2):338–49.

(44). Jiang YY, Tang GT, Zhang LH, Kong SY, Zhu SJ, Pei YY. PEGylated PAMAM dendrimers as a potential drug delivery carrier: in vitro and in vivo comparative evaluation of covalently conjugated drug and noncovalent drug inclusion complex. J. Drug Targeting. 2010; 18(5):389–403.

(45). Kane MA, Portillo RM, Elwood PC, Antony AC, Kolhouse JF. The influence of extracellular folate concentration on methotrexate uptake by human KB cells. Partial characterization of a membrane-associated methotrexate binding protein. J. Biol. Chem. 1986; 261(1):44–9. [PubMed: 3941083]

(46). Westerhof GR, Rijnboutt S, Schornagel JH, Pinedo HM, Peters GJ, Jansen G. Functional activity of the reduced folate carrier in KB, MA104, and IGROV-I cells expressing folate-binding protein. Cancer Res. 1995; 55(17):3795–802. [PubMed: 7641196]

(47). Sabharanjak S, Mayor S. Folate receptor endocytosis and trafficking. Adv. Drug Delivery Rev. 2004; 56(8):1099–109.

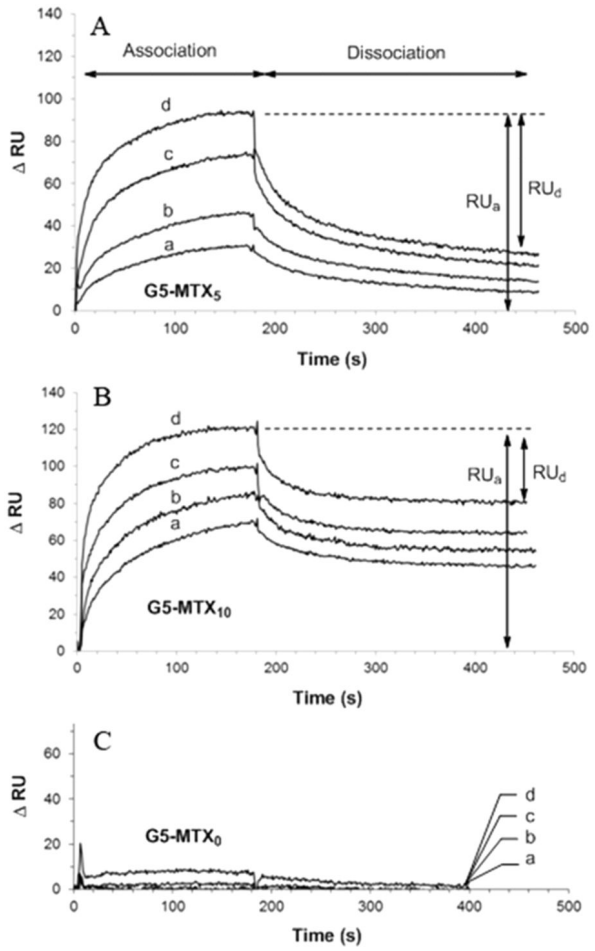

Figure 1.

Representative SPR sensograms for the dose-dependent binding of G5–MTX_5 (panel A) and G5–MTX10 (panel B) to FBP immobilized onto a CM5 sensor chip, using (a) 0.63, (b) 1.3, (c) 2.5, and (d) 5.0 μM of the conjugates. Panel C shows that "G5-Cyclooctyne Linker (G5–MTX_0)" control dendrimer that lacks any MTX failed to show any significant binding to the FBP, up to 5 μM.

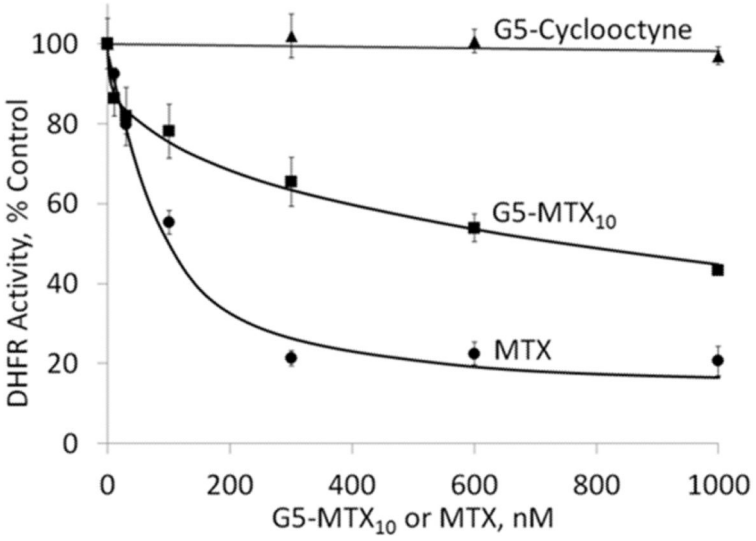

Figure 2.

Dose-dependent inhibition of recombinant DHFR by G5–MTX_{10}. The inhibition of DHFR activity by different concentrations of G5–MTX_{10} or MTX was determined as described in Materials and Methods. The data represent mean ± SE of three independent experiments. The enzyme activity is expressed as percent controls obtained in the absence of the drugs. Also shown is the lack of enzyme inhibition by the control dendrimer G5-$Cyclooctyne_{20}$, determined under similar conditions.

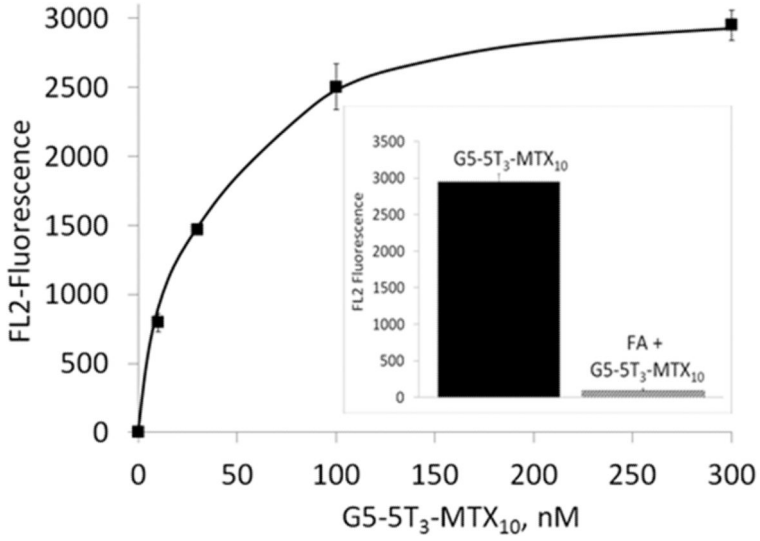

Figure 3.

Dose-dependent uptake of G5–$5T_3$–MTX_{10} into FR-expressing KB cells and the reversal of binding by free FA. Cells were treated with G5–$5T_3$–MTX_{10} for 4 h and rinsed, and the mean fluorescence of gated live cells was quantified as given in Materials and Methods. Inset: Reversal of binding of G5–$5T_3$–MTX_{10} by free FA. Cells were incubated with 300 nM G5–$5T_3$–MTX_{10} for four hours, with (filled) or without (shaded) preincubation with 15 μM FA for 30 min. The data represent background-subtracted mean ± SE of three cell samples treated with the conjugates, and each derived from the analysis of the mean fluorescence of 10,000 cells.

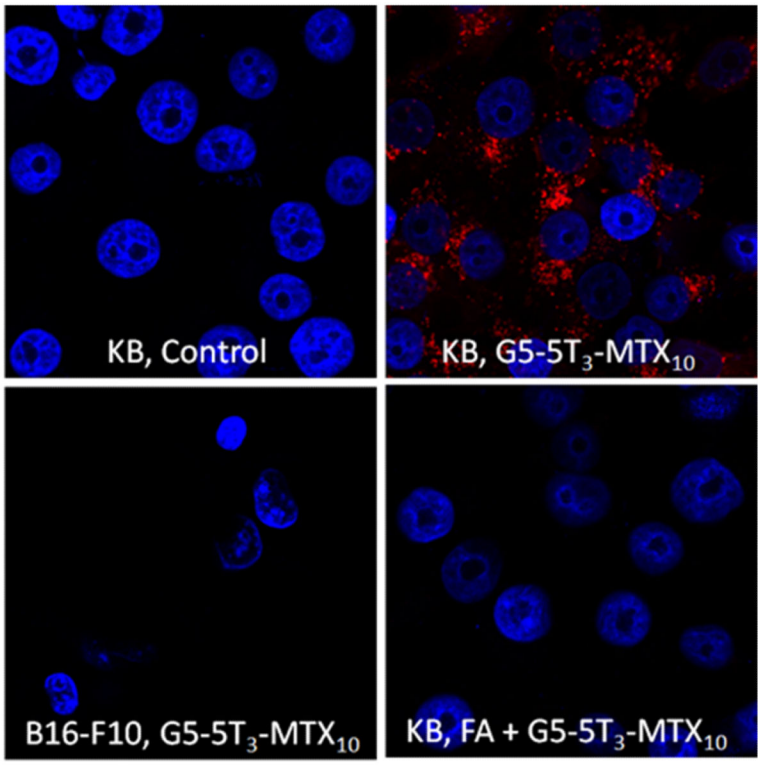

Figure 4.

Internalization of G5–$5T_3$–MTX_{10} in KB cells. FR-positive KB cells and FR-negative B16-F10 cells were treated with 300 nM G5–$5T_3$–MTX_{10} for 20 h, and confocal microscopic images were taken as described in Materials and Methods. KB cells were also pretreated with 15 μM FA for 30 min and incubated for an additional 20 h with the conjugate in the presence of the FA (bottom right panel). The data shown is representative of multiple image analysis for each set of treatment conditions.

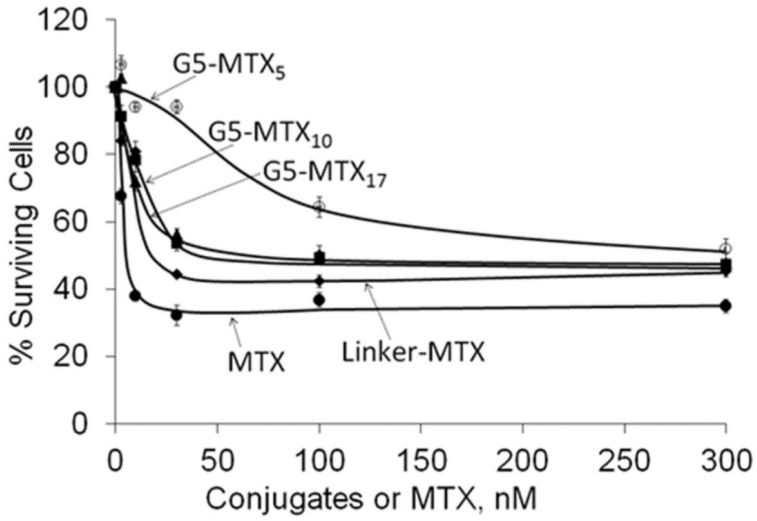

Figure 5.

Cytotoxicity of G5–MTX_n conjugates in KB cells. Cells were incubated for 48 h with the indicated conjugates, and the cytotoxicity was determined by XTT assay as given in Materials and Methods. The data represent the mean ± SE of 4 cell samples, with similar data obtained in an independent experiment. The "Linker-MTX" refers to γ-N_3-MTX, the azide-terminated MTX derivative (see Scheme 1).

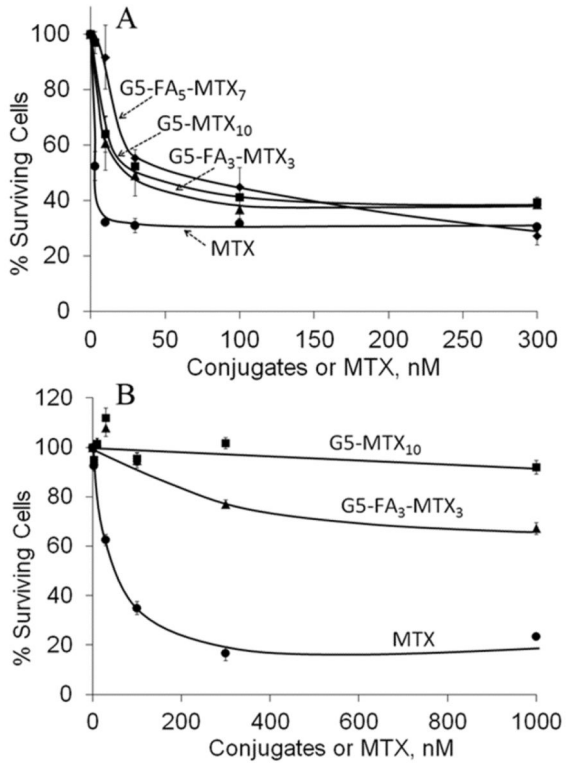

Figure 6.

Cytotoxicity of G5–MTX_{10} in FR-positive KB cells (A) vs FR-negative B16 cells (B). Also shown for comparison are the cytotoxicity of two control conjugates G5–FA_5–MTX_7 and G5–FA_3–MTX_3. Cells were incubated for 72 h with the indicated conjugates, and the cytotoxicity was determined by XTT assay, as given in Materials and Methods.

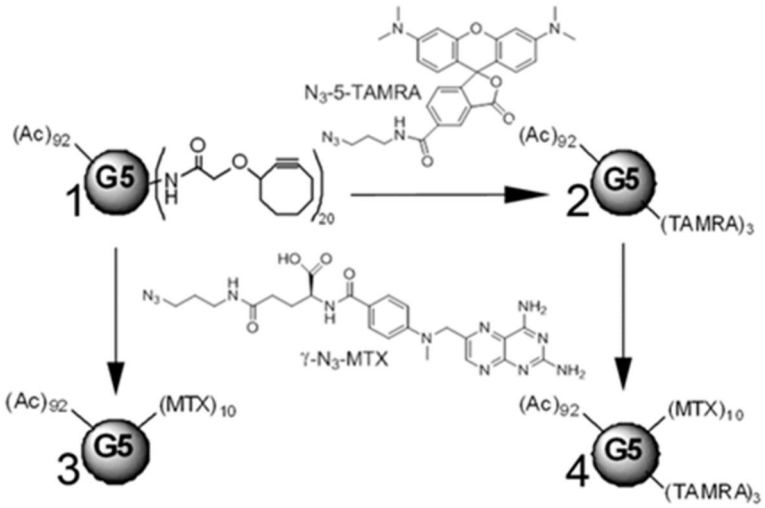

Scheme 1. Schematic Representation of the Synthesis of G5–5T$_3$ (2), G5–MTX$_{10}$ (3), and G5–5T$_3$–MTX$_{10}$ (4) from G5-Cyclooctyne$_{20}$ (1)[a]

[a]Not shown on conjugates **2**, **3**, and **4** are the remaining cyclooctyne groups following the click chemistry conjugation of the ligands.

Table 1

Rate Constants and Equilibrium Dissociation Constants (K_D) for Binding of G5–MTX_n (n = 0, 5, 10) to the Folate Binding Protein on the Surface Measured by SPR Spectroscopy

(G5–MTX_n)	k_{on} (M^{-1} s^{-1})	k_{off} [a] (s^{-1})	K_D [b] (M)	β [c]
G5–MTX_0			no binding	
G5–MTX_5	9.1(±5.4) × 10^4	2.3(±1.1) × 10^{-3}	2.8 × 10^{-8}	857 (171[d])
G5–MTX_{10}	1.2(±0.6) × 10^5	4.8(±3.9) × 10^{-4}	5.5 × 10^{-9}	4360 (436[d])

[a] An estimate based on the main dendrimer fraction for each conjugate that shows slower dissociation.

[b] Each dissociation constant ($K_D = k_{off}/k_{on}$) represents a mean value calculated by averaging the kinetic data obtained from the analysis of eight individual sensorgrams acquired at four different concentrations (5.0 to 0.63 μM; each in duplicate).

[c] β = the factor of multivalent enhanced binding = K_D^{mono}/K_D^{multi} where K_D^{mono} = 2.4 × 10^{-5} M (free MTX).

[d] valency (n)-corrected β value = (β/n) where n is equal to 5 or 10.